

Topological Properties of the Braid Stirring Pattern

Yoshihiro Yamaguchi

Teikyo Heisei University, Ichihara, Chiba 290-0170, Japan
E-mail address: chaosfractal@iCloud.com

(Received June 17, 2015; Accepted October 1, 2015)

Put several rods in the fluid and stir them with the rules of braid. A beautiful and strange stirring pattern appears on the surface of the fluid. We name this pattern “the braid stirring pattern (BSP)”. We discuss the topological properties of BSP, for example, the tunnel number, the growth rate of tunnel length, and the ratios among tunnel lengths.

Key words: Braid Stirring Pattern, Topological Chaos, Tunnel Number, Growth Rate of Tunnel Length, Ratios among Tunnel Lengths

1. Introduction

In everyday life, we pour milk into coffee in a cup, and may stir milk and coffee with a spoon. The figure appearing on the surface is an example of rod stirring pattern. Boyland, Aref and Stremler (Boyland *et al.*, 2000) published the article discussing the properties of the rod stirring pattern on the surface of viscous fluid. According to the rule of braid, they moved three rods inserted into the fluid. Here, the motion of fluid is approximately two-dimensional. They applied the braid theory to analyze the pattern on the surface of the fluid. If the braid used to stir several rods possesses a positive topological entropy, the topological chaos exists on the surface. The fluid is stirred by the rods slowly. Thus, the topological chaos is not a phenomenon caused by a turbulent flow. The chaotic trajectory is observed as the boundary curve between milk and coffee. It is stretched and folded by the fluid motion and it does not intersect itself. The boundary curve on the surface of fluid is a suitable object to study the mixing process. Changing the number of rods and the braid, the rod stirring pattern has been extensively studied (Thiffeault and Finn, 2006). In this paper, instead of “the rod stirring pattern”, we call the pattern on the surface of fluid “the braid stirring pattern (BSP)”.

Using any braid, BSP is constructed. In order to discuss the properties of BSP rigorously, it is necessary to understand the properties of braid. In this paper, we use the braid constructed by the periodic orbit in the two-dimensional area preserving map. Particularly, we use a braid β_5 constructed by the period-5 orbit.

$$\beta_5 = \sigma_4^{-1} \sigma_3^{-1} \sigma_2^{-1} \sigma_1^{-1} \sigma_4^{-1} \sigma_3^{-1}. \quad (1)$$

This is the well-known braid, which has the minimum positive topological entropy among the braids for period-5 orbits. Here the notation σ_k^{-1} represents the generator of braid (Murasugi, 1996). We study the geometrical and algebraic properties of BSP constructed by β_5 .

In Sec. 2, we explain the origin of β_5 and how to make BSP. In Sec. 3, the geometrical and algebraic properties of BSP are discussed. Our results are summarized in Sec. 4.

2. Braid Stirring Pattern

2.1 Origin of the braid β_5

First, we explain the origin of braid β_5 , briefly. We use the two-dimensional area preserving map T in the Hénon family (Yamaguchi and Tanikawa, 2009, 2011).

$$y_{n+1} = y_n + f_a(x_n), \quad (2)$$

$$x_{n+1} = x_n + y_{n+1}. \quad (3)$$

Here, $f_a(x) = a(x - x^2)$, and $a(\geq 0)$ is a parameter. At $a > 0$, two fixed points $P = (0, 0)$ and $Q = (1, 0)$ exist. The fixed point P is a saddle point. The other one Q is an elliptic orbit at $0 < a < 4$, and a saddle with reflection at $a > 4$. All orbits except for P and Q rotate around Q clockwise. There are two symmetry axes S_h ($y = 0$) and S_g ($y = -f_a(x)/2$) (see Fig. 1). At $a \geq 5.1766 \dots$, there exists the Smale horseshoe in the phase space (Devaney, 2003; Yamaguchi and Tanikawa 2009, 2011). Thus, the topological entropy of T is less than or equal to $\ln 2$.

At $a = 5.1192 \dots$, the saddle-node bifurcation occurs, and two periodic orbits with the rotation number $2/5$ appear. These orbits rotate around Q twice during one period. In Fig. 1, the saddle orbit is depicted. Using the orbital points rotating around Q clockwise, the braid is constructed (Fig. 2). We set two planes. Every strand starts from the upper plane representing the configuration at $t = 0$ and arrives at the lower plane representing the configuration at $t = 1$. In order to understand the movement of strands, we add the strand of Q illustrated by thick line in Fig. 2. Rotating around the thick strand, every strand goes down. For example, the strand from z_2 to z_3 passes backside of thick strand and the strand from z_3 to z_4 passes in the front of the thick strand. Finally, we delete the thick strand, and obtain the braid β_5 depicted in Fig. 3.

We explain the properties of periodic orbit depicted in Fig. 1. We stand at Q and observe the orbit. The polar-

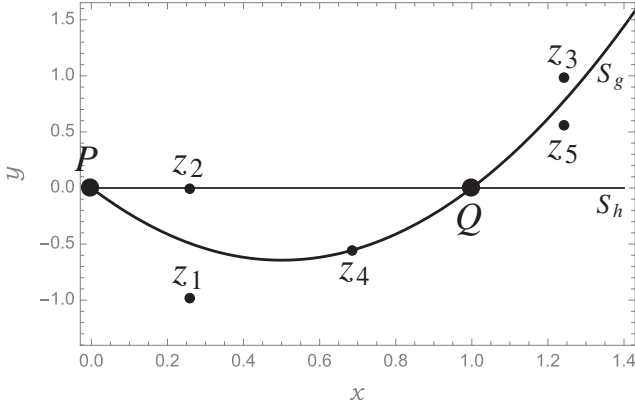


Fig. 1. Saddle periodic orbit with rotation number $2/5$ where $z_1 = Tz_5$, $z_2 = Tz_1$, $z_3 = Tz_2$, $z_4 = Tz_3$, and $z_5 = Tz_4$. This orbit rotates around Q twice during one period. The orbital point z_2 locates on S_h , and z_4 locates on S_g . $a = 5.15$.

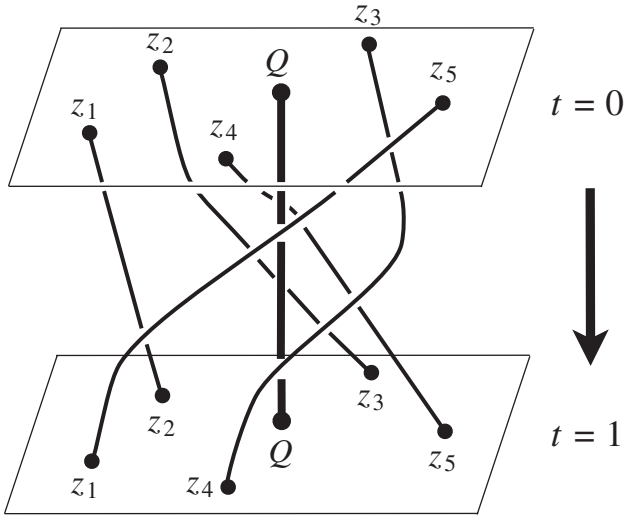


Fig. 2. How to make the braid β_5 . The upper plane represents the configuration at $t = 0$ and the lower one represents the configuration at $t = 1$. Thick arrow represents the direction of the time evolution. For example, the strand starts at z_1 in the upper plane goes down and arrives at z_2 in the lower plane. The thick strand starts at Q in the upper plane goes down and arrives at Q in the lower plane. Each strand rotates around thick strand and goes down.

coordinate representation (θ_k, r_k) is used. Here, we measure an angle clockwise from the segment QP . We observe the angular velocities of the orbital points from $z_1 = (\theta_1, r_1)$ to $z_4 = (\theta_4, r_4)$. During three iterations, the orbit rotates around Q approximately once ($\theta_4 - \theta_1 \approx 2\pi$). The orbit from z_1 to z_4 rotates slowly. On the other hand, during two iterations, the orbit from z_4 to z_1 rotates around Q approximately once. Thus, the orbit from z_4 to z_1 rotates rapidly.

The slow rotation is characterized by the rotation number $1/3$ and the rapid one by the rotation number $1/2$. Thus, the total rotation is characterized by the rotation number $2/5$, which is divided as follows.

$$\frac{2}{5} = \frac{1+1}{3+2} \equiv \frac{1}{3} \circ \frac{1}{2}. \quad (4)$$

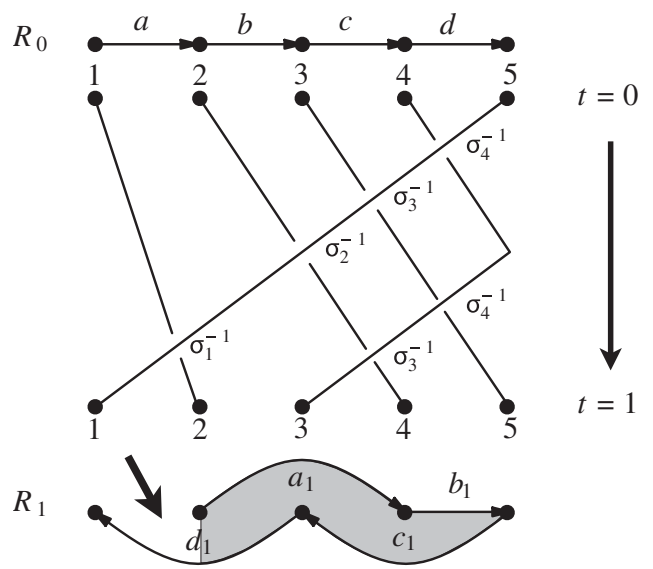


Fig. 3. Braid β_5 . The upper region of braid represents the configuration at $t = 0$ and the lower one the configuration at $t = 1$. Time flows from the upper region to the lower one (see thick arrow). Let R_0 be the set of Strings $\{a, b, c, d\}$ located above the braid, and R_1 be the set of Strings $\{a_1 = \beta_5 a, b_1 = \beta_5 b, c_1 = \beta_5 c, d_1 = \beta_5 d\}$ located below the braid. Thick arrow in R_1 represents the entrance of tunnel (gray region). Here, σ_k^{-1} ($k = 1, 2, 3, 4$) are the generators to represent the braid.

In the situation that the periodic orbit satisfying Eq. (4) exists, there exists the periodic orbit with the rotation number $1/3$ and that with the rotation number $1/2$ (Yamaguchi and Tanikawa, 2009, 2011). In fact, the former orbit appears at $a = 3$ through the rotation bifurcation of Q . At $a = 3$, two periodic orbits appear. One orbit is an elliptic orbit and the other one is a saddle orbit. At $a = 4$, the periodic orbit with the rotation number $1/2$ appears through the period-doubling bifurcation of Q . The periodic orbit rotates about 180 degree per one iteration around Q . Using the coexistence of the saddle periodic orbit with rotation number $1/3$ and the periodic orbit with rotation number $1/2$, we discuss the properties of BSP in Subsec. 3.1.

2.2 Braid and braid stirring pattern

Using the braid $\beta_5 = \sigma_4^{-1} \sigma_3^{-1} \sigma_2^{-1} \sigma_1^{-1} \sigma_4^{-1} \sigma_3^{-1}$, we explain how to make BSP. All strands go down from the upper plane to the lower one (Fig. 3). Time progresses towards the lower plane from the upper one and the inverse progress never occur. The braid β_5 means the action to describe the time evolution.

Let the positions at which the strands start be Position P_k ($k = 1, 2, \dots, 5$). In Fig. 3, the abbreviated notations 1, 2, 3, 4 and 5 are used. In fact, the first strand starts at Point 1 and reaches at Point 2, the second one starts at Point 2 and reaches at Point 4, and so on.

In order to reproduce the pattern of boundary curve on the surface of fluid, we prepare the four strings. At $t = 0$, we set String a connecting from Point 1 to Point 2. Similarly, we also set String b , String c , and String d . These lengths are assumed to be one. These are deformed by the action of β_5 . Let R_0 be the set of Strings $\{a, b, c, d\}$. In the following, we study the structure of $R_k = \beta_5^k R_0$ ($k \geq 0$), which inherits the properties of β_5 .

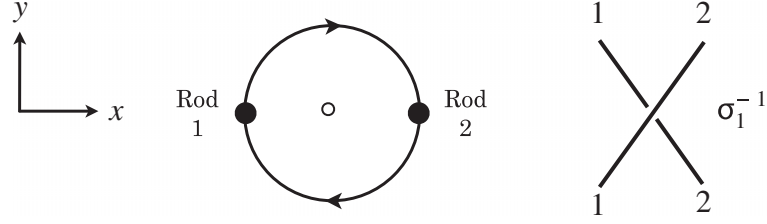


Fig. 4. Two rods named Rod 1 located at Point 1 and Rod 2 located at Point 2 are observed from the top. Around the center illustrated by a circle, two rods rotate 180 degrees clockwise. This process is represented by the generator σ_1^{-1} .

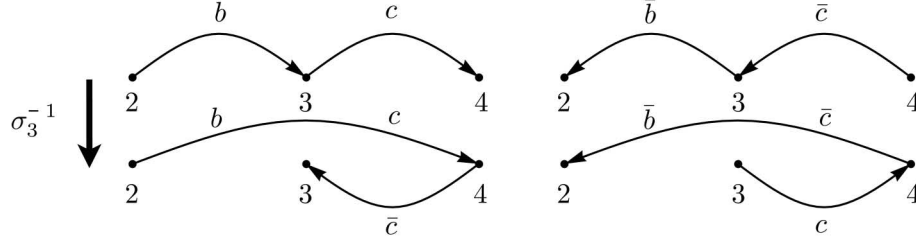


Fig. 5. Operating σ_3^{-1} on bc , the clockwise turn occurs at Point 4 (Left figure). Operating σ_3^{-1} on $\bar{c}\bar{b}$, the counterclockwise turn occurs at Point 4 (right figure).

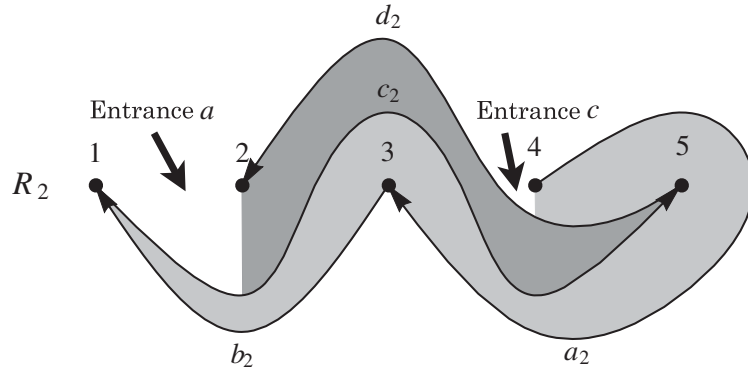


Fig. 6. $BSP:R_2$. There exist two entrances named Entrances a and c . Note that $a_2 = \beta_5 a_1 = \beta_5^2 a$.

We define the x -axis along the direction from Point 1 to Point 2 and the y -axis perpendicular to the x -axis. Here, the x - y plane expresses the surface of fluid. Rod 1 and Rod 2 rotate 180 degrees clockwise around a circle between two rods (see Fig. 4). It is noted that all rods rotate clockwise. Operating β_5 on the rods, the fluid around these rods are dragged to the x -direction and to the y -direction. The movement along the y -direction naturally gives rise to the expansion of R_k . In order to study the geometrical properties of BSP, we need the expansion along the y -axis of R_k . On the other hand, when we investigate the algebraic properties, we need only the stretching and shrinking of Strings $\{a, b, c, d\}$ along the x -axis.

Under the braid in Fig. 3, R_1 is shown. Next, we draw R_2 . By the action β_5 , the image of Point k ($1 \leq k \leq 5$) is determined. The image of Point 1 is Point 2. This transition is represented as $1 \rightarrow 2$. Here, we set the vector A at Point 1 perpendicularly. The direction of $\beta_5 A$ and that of A are the same. In order to represent this fact, the transition is represented as $\bar{1} \rightarrow \bar{2}$ and $\underline{1} \rightarrow \underline{2}$. Next, we consider

the transition $4 \rightarrow 3$. We also set the vector B at Point 4 perpendicularly. The direction of $\beta_5 B$ and that of B are reverse. Thus, the transition is represented as $\bar{4} \rightarrow \bar{3}$ and $\underline{4} \rightarrow \underline{3}$. The images of all points are obtained.

Rule I.

$$\bar{1} \rightarrow \bar{2}, \quad \underline{1} \rightarrow \underline{2}, \quad (5)$$

$$\bar{2} \rightarrow \bar{4}, \quad \underline{2} \rightarrow \underline{4}, \quad (6)$$

$$\bar{3} \rightarrow \bar{5}, \quad \underline{3} \rightarrow \underline{5}, \quad (7)$$

$$\bar{4} \rightarrow \bar{3}, \quad \underline{4} \rightarrow \underline{3}, \quad (8)$$

$$\bar{5} \rightarrow \bar{1}, \quad \underline{5} \rightarrow \underline{1}. \quad (9)$$

If the image passes the upper (lower) region of Point k , we represent this fact as \bar{k} (\underline{k}). The image of String a is $a_1 = bc$. The image bc passes the upper region of Point 3. Adding this information, $a_1 = b\bar{3}c$ is given. The other images are similarly defined. The rules for four strings are obtained.

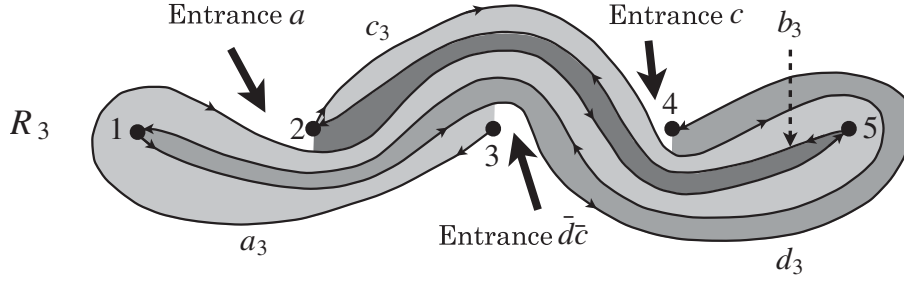


Fig. 7. BSP: R_3 . There exist three entrances.

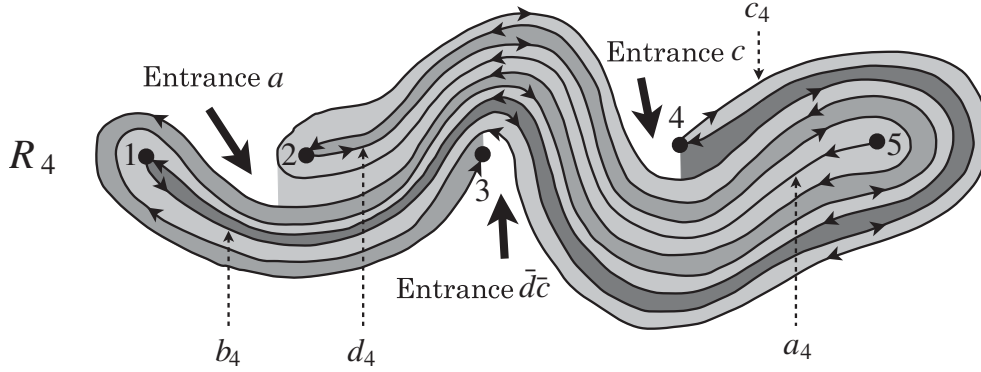


Fig. 8. BSP: R_4 . There exist three entrances.

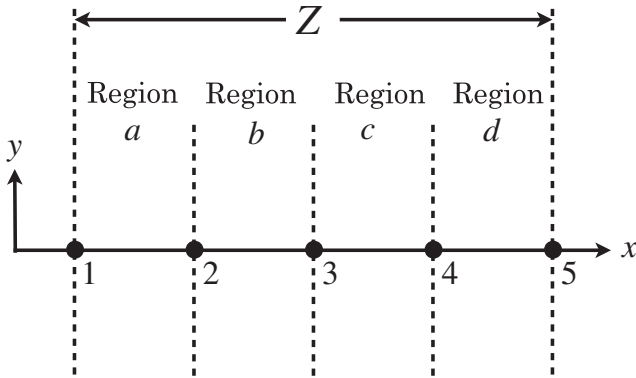


Fig. 9. Definitions of Region a , Region b , Region c , Region d , and the fundamental region Z in the x - y plane representing the surface of fluid. Symbol k ($k = 1, 2, \dots, 5$) represents Point k .

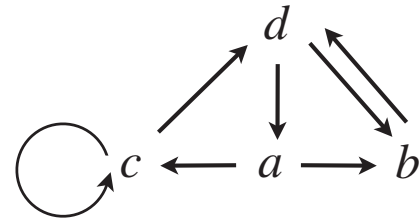


Fig. 10. Transitions among Regions (Strings) $\{a, b, c, d\}$, where a represents Region a , b represents Region b , and so on.

Rule II.

$$a_1 = b\bar{3}c, \tag{10}$$

$$b_1 = d, \tag{11}$$

$$c_1 = d\bar{4}\bar{c}, \tag{12}$$

$$d_1 = \bar{b}\bar{2}\bar{a}. \tag{13}$$

Here, $a_1 = \beta_5 a$, $b_1 = \beta_5 b$, $c_1 = \beta_5 c$, $d_1 = \beta_5 d$. For example, $\bar{4}$ in c_1 means that the image c_1 passes the lower region of Point 4. The orientation of c and that of d are right, and the orientation of \bar{c} and that of \bar{d} are left.

First, we study $a_2 = \beta_5 a_1 = \beta_5^2 a$. By Rules I and II, the image $a_2 = d\bar{5}\bar{d}\bar{4}\bar{c}$ is obtained. Here, we use the fact that

the image of $\bar{3}$ is $\bar{5}$ (see Eq. (7)). It is noted that the relations of right and left and the vertical relations do not change during the transition from $\bar{3}$ is $\bar{5}$. Omitting two numerals included in $d\bar{5}\bar{d}\bar{4}\bar{c}$, $d\bar{d}\bar{c}$ is obtained. Thus, the length of image is three. Repeating this procedure, the length of image a_k is calculated.

Next, consider $c_1 = \beta_5 c$. Operate β_5 on $c_1 = d\bar{4}\bar{c}$. We use the relation $\beta_5 d = a\bar{2}b$. This means that the image $\beta_5 d$ passes the lower region of Point 2 from the right side of Point 2 to the left side. When Point 3 is mapped to Point 4, the image turns 180 degree clockwise. Thus, the vertical relation reverses. The fact mentioned here is represented as $\bar{4} \rightarrow \bar{3}$ (see Eq. (8)). Finally, using $\beta_5 \bar{c} = c\bar{4}d$, we obtain the representation of c_2 . We summarize the results.

$$a_2 = d\bar{5}\bar{d}\bar{4}\bar{c}, \tag{14}$$

$$b_2 = \bar{b}\bar{2}\bar{a}, \tag{15}$$

$$c_2 = a\bar{2}b\bar{3}c\bar{4}d, \tag{16}$$

$$d_2 = \bar{d}\bar{4}\bar{c}\bar{3}\bar{b}. \tag{17}$$

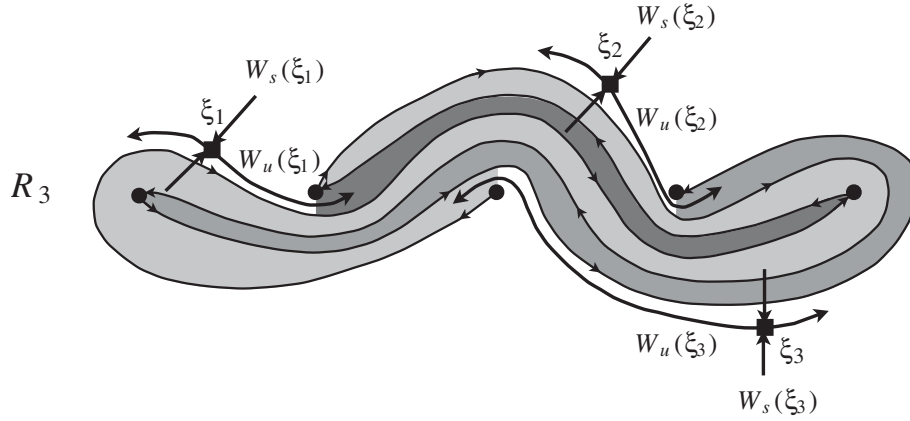


Fig. 11. The saddle periodic orbit with rotation number $1/3$, where $\xi_1 = \beta_5 \xi_3$, $\xi_2 = \beta_5 \xi_1$, and $\xi_3 = \beta_5 \xi_2$. The orbital point ξ_1 exists in Regions a at $y > 0$, ξ_2 in Region c at $y > 0$ and ξ_3 in Region d at $y < 0$, where $W_s(\xi_k)$ ($k = 1, 2, 3$) is the stable manifold of ξ_k and $W_u(\xi_k)$ is the unstable manifold of ξ_k . The unstable manifolds penetrate into R_3 from the entrances.

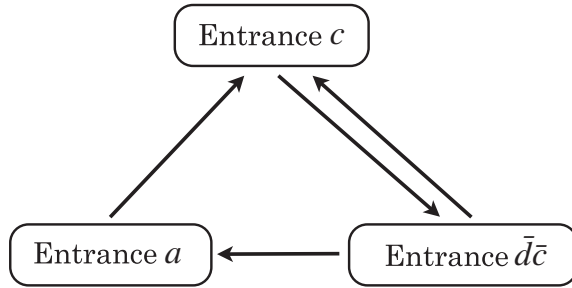


Fig. 12. Transitions among three entrances.

Combining these images, we obtain the notation for R_2 .

$$R_2 : d\bar{5}\bar{d}4\bar{c}\bar{b}2\bar{a}a2\bar{b}3\bar{c}4\bar{d}\bar{d}4\bar{c}\bar{3}\bar{b}. \quad (18)$$

In order to draw the figure of R_2 , we start from Point 4 and draw the curve represented by d , which is the first symbol of R_2 . We reach at Point 5 and rotate around Point 5 clockwise due to $\bar{5}$ in $d\bar{5}\bar{d}$.

We reach at Point 4, pass the lower region of Point 4, and reach at Point 3. Next, we pass the lower region of Point 2, and go forward Point 1. We encounter $\bar{a}a$ included in R_2 . Therefore, we turn clockwise or counterclockwise at Point 1, and go toward Point 2. We have to determine how to turn at Point 1.

Remember the fact that two rods rotate clockwise by the generator. We operate σ_3^{-1} on Strings b and c facing right. Thus, the clockwise turn occurs at Point 4 (see the left figure of Fig. 5). We operate σ_3^{-1} on Strings \bar{b} and \bar{c} facing left. Thus, the counterclockwise turn occurs at Point 4 (see the right figure of Fig. 5). These imply that the way of the turn at the point is decided by the direction of original string.

We remark that \bar{a} in $\bar{a}a$ is a part of image of d . The direction of d is right. Thus, \bar{a} is the image of string facing right. As a result, the clockwise turn occurs at Point 1.

We go to Point 2, pass the lower region of Point 2, and pass the upper region of Point 3. If we pass the upper region of Point 4, the image c_2 intersects the image a_2 . Thus, we pass the lower region of Point 4 and reach at Point 5. At Point 5, we determine how to turn. Since d in $d\bar{d}$ is a part of

the image of \bar{c} , the counterclockwise turn occurs at Point 5. We pass the lower region of Point 4, pass the upper region of Point 3 and reach at Point 2. Thus, the figure of R_2 in Fig. 6 completes. Using the procedure mentioned here, we can draw the figures of R_3 and R_4 (see Figs. 7 and 8).

3. Properties of BSP

3.1 Geometrical properties of BSP

Thick arrows illustrated in Figs. 6,7 and 8 represent the entrances. The fluid flows into R_k from the entrances. The fluid flowing into R_k is stretched and folded in R_k . This is a typical chaotic process (Devaney, 2003).

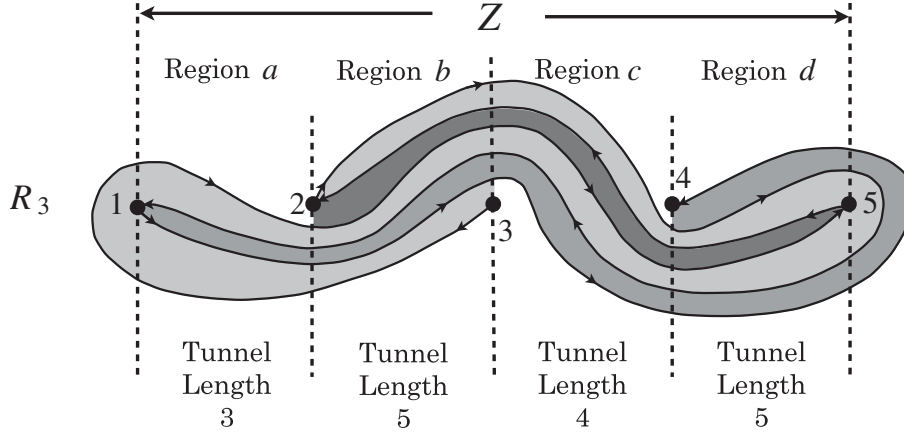
Here, we discuss the number of entrances. In R_1 , there exists only one entrance. Another entrance appears in R_2 , and the third entrance appears in R_3 . New entrance does not appear in R_4 . Thus, there exist three entrances and three tunnels in R_k ($k \geq 4$). The number of entrances (tunnels) is the quantity characterizing BSP.

We define Region a in the x - y plane at which String a exists (see Fig. 9). We draw a dotted line along the y direction passing through Point 1. For the other points, we draw dotted lines. Region a is an open area sandwiched by the dotted line passing through Point 1 and by that passing through Point 2. Similarly, Regions b , c and d are defined. The open region between the dotted line passing through Point 1 and that passing through Point 5 is the fundamental region Z . For example, the portion of R_2 extends outside the fundamental region Z . The left and right regions outside Z contribute the folding effect. However, these portions do not contribute the algebraic properties discussed here.

Using Eqs. (10)–(13), we define the transition matrix M among Regions a , b , c and d .

$$M = \begin{pmatrix} a & b & c & d \\ a & 0 & 1 & 1 & 0 \\ b & 0 & 0 & 0 & 1 \\ c & 0 & 0 & \bar{1} & \bar{1} \\ d & \bar{1} & \bar{1} & 0 & 0 \end{pmatrix}. \quad (19)$$

Here, a in M is the abbreviation of Region a or String a . The first column means that the image of Region a covers Region b and Region c . The symbol 1 means the admissible

Fig. 13. Tunnels in R_3 .

transition and the symbol 0 the inhibited one. The image of Region c covers Region c and Region d inversely. Similarly, the image of Region d covers Region b and Region a inversely. The symbol $\bar{1}$ in M represents the inverse cover.

The transitions among Regions (Strings) are depicted in Fig. 10. For example, the transitions from a to b and c are admissible. From Fig. 10, we obtain that there exist two period-3 orbits.

$$a \rightarrow b \rightarrow d \rightarrow a, \quad a \rightarrow c \rightarrow d \rightarrow a. \quad (20)$$

Taking into account the covering direction, the first transition is rewritten as

$$a \rightarrow b \rightarrow d \rightarrow \bar{a} \rightarrow \bar{b} \rightarrow \bar{d} \rightarrow a. \quad (21)$$

The second one is rewritten as

$$a \rightarrow c \rightarrow \bar{d} \rightarrow a. \quad (22)$$

After the one period, the direction around a in Eq. (21) is inverted. Therefore, Eq. (21) represents the elliptic periodic orbit or the saddle periodic orbit with reflection, and Eq. (22) represents the saddle periodic orbit.

The transition

$$b \leftrightarrow d \quad (23)$$

represents the period-2 orbit. Taking into account the covering direction, this transition is rewritten as

$$b \rightarrow d \rightarrow \bar{b} \rightarrow \bar{d} \rightarrow b. \quad (24)$$

This implies that this periodic orbit is the elliptic periodic orbit or the saddle orbit with reflection.

If the orbital points are located near the unstable manifold of saddle point, these points flow along the unstable manifold. Thus, the saddle point makes the entrance of fluid. The first entrance named Entrance a appears at Region a at $y > 0$ (see Fig. 3). The image of Region a is located at Region c at $y > 0$. Thus, Entrance c appears at Region c at $y > 0$ (see Fig. 6). The third entrance exists Region c at $y < 0$ in Fig. 7. However, the image of Region c does not cover Region a (see Fig. 10). We can reconsider that

Table 1. Increasing of tunnel lengths.

k	L_{3k}^a	L_{3k}^c	$L_{3k}^{d\bar{c}}$	L_{3k}
1	3	5	9	17
2	18	31	54	103
3	95	164	283	542
4	489	843	1452	2784
5	2502	4310	7422	14234
6	12783	22015	37911	72709

the third entrance extends over Regions c and d at $y < 0$. As a result, Region d at $y < 0$ is mapped at Region a at $y > 0$, and Region c at $y < 0$ is mapped at Region c at $y > 0$. Thus, let Entrance $\bar{d}\bar{c}$ be the third entrance. Hence, the saddle point ξ_1 exists in Region a at $y > 0$, ξ_2 in Region c at $y > 0$, and ξ_3 in Region d at $y < 0$ (see Fig. 11). The existence of saddle points is consistent with that of entrances. We remark that this saddle orbit has the rotation number $1/3$.

The relations among three entrances are summarized in Fig. 12. Three entrances exist in R_k ($k \geq 4$), and three tunnels exist in R_k ($k \geq 4$). We call the tunnel with Entrance a \mathcal{T}_a . Similarly, \mathcal{T}_c and $\mathcal{T}_{\bar{d}\bar{c}}$ are used.

3.2 Algebraic properties of BSP

Using the properties of transition matrix M , the algebraic properties of BSP are determined. The eigenvalue function

$$\lambda^4 - \lambda^3 - \lambda^2 - \lambda + 1 = 0 \quad (25)$$

is obtained. Solutions are 1.72208 , 0.58069 , and $-0.65138 \pm 0.75874i$. Let the maximum value be $\lambda_{max} = 1.72208$ called a line-stretching factor. Thus, the lower bound for the topological entropy is $\ln \lambda_{max}$. If the system has the braid β_5 , the topological entropy of the system is larger than or equal to $\ln \lambda_{max}$. Thus, the chaos characterized by the braid is called the topological chaos (Boyland *et al.*, 2000). This chaos is determined by only the braid.

Using the transition matrix M^3 , we calculate the tunnel

length.

$$M^3 = \begin{pmatrix} | & a & b & c & d \\ a & 2 & 2 & 1 & 1 \\ b & 0 & 1 & 1 & 1 \\ c & 1 & 2 & 2 & 2 \\ d & 1 & 1 & 1 & 2 \end{pmatrix}. \quad (26)$$

Comparing Eq. (26) and Fig. 13, we can understand how to calculate the tunnel length. The total summation in the first row of M^3 is 4. This is the number of the images of Strings a, b, c and d returning to Region a . Thus, in Region a , there exist three tunnels. Each length is one and total length is three. Similarly, there exist five tunnels in Region b , four tunnels in Region c , and five tunnels in Region d . Summing up these lengths, we obtain the total length $L_3 = 17$ in R_3 . Let m_{3k} be the summation of elements in M^{3k} , and L_{3k} be the total length of tunnels in R_{3k} . We obtain the relation

$$L_{3k} = m_{3k} - 4. \quad (27)$$

The image of the first entrance represented by Entrance a is located in Region b and c . For simplicity, we write this image as bc . In the image bc , c represents Entrance c . Omitting b in bc , we calculate the expansion of the rest part c . Operating β_5^2 on c , we have $abcd$. In this notation, a represents Entrance a . Therefore, omitting the first symbol a , we get bcd , which represents the tunnel whose entrance is Entrance a . Thus, the tunnel length is three.

Next, we study the image of Entrance c . We obtain $\beta_5^3 c = bcd\bar{d}\bar{c}\bar{b}\bar{a}$, and omit bc . Thus, the rest part $d\bar{d}\bar{c}\bar{b}\bar{a}$ represents the tunnel. The tunnel length is five. Finally, we obtain $\beta_5^3 \bar{d}\bar{c} = d\bar{d}\bar{c}\bar{b}\bar{a}bcd\bar{d}\bar{c}\bar{b}$. Omitting $d\bar{d}\bar{c}$, we have $\bar{b}\bar{a}abcd\bar{d}\bar{c}\bar{b}$. The tunnel length is 9. Repeating this procedure, the lengths L_{3k}^a , L_{3k}^c , and $L_{3k}^{\bar{d}\bar{c}}$ of tunnels \mathcal{T}_a , \mathcal{T}_c , and $\mathcal{T}_{\bar{d}\bar{c}}$ are calculated (see Table 1).

Using the data for large k , we determine the average expansion rate of the tunnel length. Summation of all elements in M^{3k} diverges as λ_{max}^{3k} . Let L_k be the total tunnel length in R_k . After one operation β_5 , the total tunnel length

in R_{k+1} is about $L_{k+1} \approx \lambda_{max} \times L_k$. The average expansion rate for each tunnel is also λ_{max} .

For the tunnels \mathcal{T}_a , \mathcal{T}_c , and $\mathcal{T}_{\bar{d}\bar{c}}$, we obtain the relations:

$$\mathcal{T}_c = \beta_5 \mathcal{T}_a, \quad \mathcal{T}_{\bar{d}\bar{c}} = \beta_5 \mathcal{T}_c. \quad (28)$$

Thus, Eq. (29) holds for large value of k .

$$L_{3k}^a : L_{3k}^c : L_{3k}^{\bar{d}\bar{c}} = 1 : \lambda_{max} : \lambda_{max}^2. \quad (29)$$

Using the data for $k = 6$ in Table 1, we confirm these ratios.

$$\lambda_{max} \times 12783 = 22013.3 \approx 22015,$$

$$\lambda_{max} \times 22015 = 37911.6 \approx 37911.$$

4. Concluding Remarks

We summarize our results.

[1] The topological chaos appears in BSP constructed by the repetitive action of braid β_5 . Drawing BSP by hand, we can experience the stretching and folding processes, which are the essential properties of chaos.

[2] If the non-uniform rotation induced by the action of braid β_5 is separated into the rapid rotation and the slow one, the rapid rotation contributes the stirring effect of fluid and the slow one determines the tunnel number. The tunnel number affects the amount of fluid sucked into R_k . Combining these effects, the efficiency of mixing is determined.

[3] There exist three tunnels in BSP constructed by β_5 , and the enlargement of tunnel lengths is determined by the line-stretching factor λ_{max} .

References

- Boyland, P., Aref, H. and Stremmer, M. A. (2000) Topological fluid mechanics of stirring, *J. Fluid Mech.*, **403**, 277–304.
- Devaney, R. (2003) *An Introduction to Chaotic Dynamical Systems*, Westview Press.
- Murasugi, K. (1996) *Knot Theory and Its Applications*, Birkhäuser.
- Thiffeault, J.-L. and Finn, M. D. (2006) Topology, braids, and mixing in fluids, *Phil. Trans. R. Soc. Lond.*, **A364**, 3251–3266.
- Yamaguchi, Y. and Tanikawa, K. (2009) A new interpretation of the symbolic codes for the Hénon map, *Prog. Theor. Phys.*, **122**, 569–609.
- Yamaguchi, Y. and Tanikawa, K. (2011) A new interpretation of the symbolic codes for the Hénon map. II, *Prog. Theor. Phys.*, **125**, 435–471.